

Influence of damp heat testing on the electrical characteristics of $\text{Cu}(\text{In,Ga})(\text{S,Se})_2$ solar cells

C. Deibel^{a,*}, V. Dyakonov^a, J. Parisi^a, J. Palm^b, S. Zweigart^b, F. Karg^b

^aDepartment of Energy and Semiconductor Research, Faculty of Physics, University of Oldenburg, 26111 Oldenburg, Germany

^bSiemens & Shell Solar GmbH, 81739 München, Germany

Abstract

The influence of accelerated stress testing on the electrical properties of $\text{Cu}(\text{In,Ga})(\text{S,Se})_2$ thin-film solar cells is presented. Although encapsulated modules are stable, extended exposure of unencapsulated cells to damp heat (144 h, 264 h and 438 h) at 85°C and 85% humidity leads to a reduction of the fill factor and the open-circuit voltage. We further analyzed these changes by applying admittance spectroscopy, deep-level transient spectroscopy and current–voltage measurements. Damp heat stress reduces the net doping concentration of the absorber material and shifts a dominant defect state close to or at the buffer/absorber interface to higher activation energies. By comparing experimentally observed changes with the SCAPS device simulation program several possible causes for the observed changes in electrical properties are discussed: decrease of ZnO resistivity; decrease of the density of interface states; increase of shallow acceptor concentration and the introduction of deep acceptors in the $\text{Cu}(\text{In,Ga})(\text{S,Se})_2$ absorber. © 2002 Elsevier Science B.V. All rights reserved.

Keywords: $\text{Cu}(\text{In,Ga})(\text{S,Se})_2$; Solar cells; Stability; Damp heat test

1. Introduction

The long-term stability of solar cells is crucial for their success as a source of renewable energy. Encapsulated $\text{Cu}(\text{In,Ga})(\text{S,Se})_2$ thin film modules have shown stable performance over many years under outdoor conditions. Unencapsulated circuits and cells, however, show decreases in fill factor and open circuit voltage after accelerated stress testing, i.e. at high temperature (85°C) and humidity (85%). The acceleration factor of this stress test relative to a field test is presently still unknown. It would be needed for reliable extrapolations of the module lifetime based on stress test results. For this purpose, a better understanding of stress test-induced changes in the device and their associated activation energy is required.

Damp heat-induced changes in the cell I/V characteristic have been earlier attributed to modifications in

the ZnO-window layer [1] and the CIGS-absorber [2]. The present study investigates the influence of accelerated stress tests on unencapsulated ZnO/CdS/ $\text{Cu}(\text{In,Ga})(\text{S,Se})_2$ solar cells focusing on the CIGSSe absorber and the interface between window and absorber.

2. Experimental

The investigated samples consisted of open ZnO/CdS/ $\text{Cu}(\text{In,Ga})(\text{S,Se})_2$ solar cells fabricated by rapid thermal processing (RTP) of stacked elemental layers [3]. Stress testing was performed under damp heat (DH) conditions at 85% relative humidity and 85°C for test periods of 24 h, 144 h, 264 h and 438 h. The process sequence of one set of samples was interrupted after the RTP for a DH exposition of the absorber layer. After 24 h in DH the cell process was continued. We will denote these samples as absorber DH samples, cells exposed to DH as whole devices will be called DH samples, and the untreated cells will be named as-grown or reference samples. We characterized the cells using

* Corresponding author. Tel: +49-441-798-3991; fax: +49-441-798-3990.

E-mail address: deibel@ehf.uni-oldenburg.de (C. Deibel).

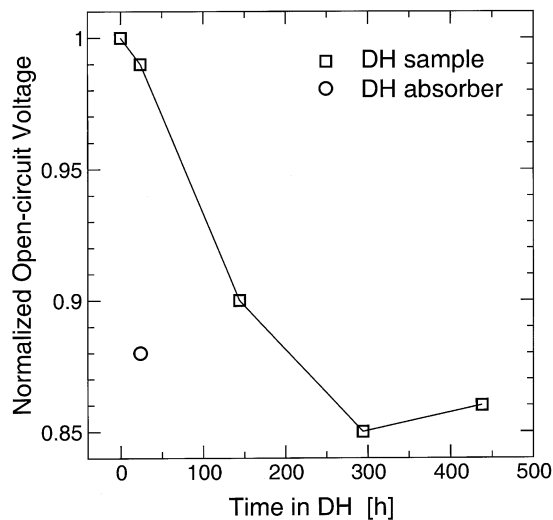


Fig. 1. Open-circuit voltage of the CIGS_{Se} cells (25°C, AM1.5) vs. time elapsed in DH.

current–voltage measurements under AM1.5 illumination admittance spectroscopy (Solartron 1260) and deep-level transient spectroscopy (DLTS, Semitrap 82E). Temperature-dependent measurements were performed using a helium closed-cycle cryostat.

2.1. Current–voltage characteristics

Devices exposed to DH conditions show decreases in fill factor and the open-circuit voltage (see Fig. 1) whereas the short-circuit current remains constant. Wen-

nerberg et al. [1] investigated the role of the ZnO window layer in DH degradation and point out that it can partially explain the increasing series resistance. A second contribution may originate from the window/absorber interface, the absorber bulk or the back contact. An extrapolation of the open-circuit voltage vs. temperature to 0 K yields the CIGS_{Se} bandgap as activation energy. This result is in accordance with observations by Schmidt et al. [2], i.e. recombination in the space charge region is dominant before and after DH.

2.2. Capacitance spectroscopy

Capacitance–voltage measurements (performed at $T=90$ K and $f=100$ kHz to include only the response of the shallow acceptors) reveal that the net doping density of the CIGS_{Se} absorber decreases due to DH. As-grown samples show free hole concentrations of approximately $5.5 \cdot 10^{15} \text{ cm}^{-3}$. After 144 h of DH treatment this value is reduced to $2.5 \cdot 10^{15} \text{ cm}^{-3}$. The absorber DH sample shows a net doping density of $1.5 \cdot 10^{15} \text{ cm}^{-3}$. The activation of shallow acceptors can be observed in the admittance (see Fig. 2), where they are represented by a characteristic capacitance step α . The change of the absolute capacitance values indicates a strong increase in the space charge (SC) width due to DH in accordance with the decrease in net doping density. As-grown samples have a SC width of approximately 300 nm, which becomes more than 600 nm wide after 144 h of DH.

A second capacitance step β can be seen in Fig. 2. Reverse-DLTS measurements confirm that this minority

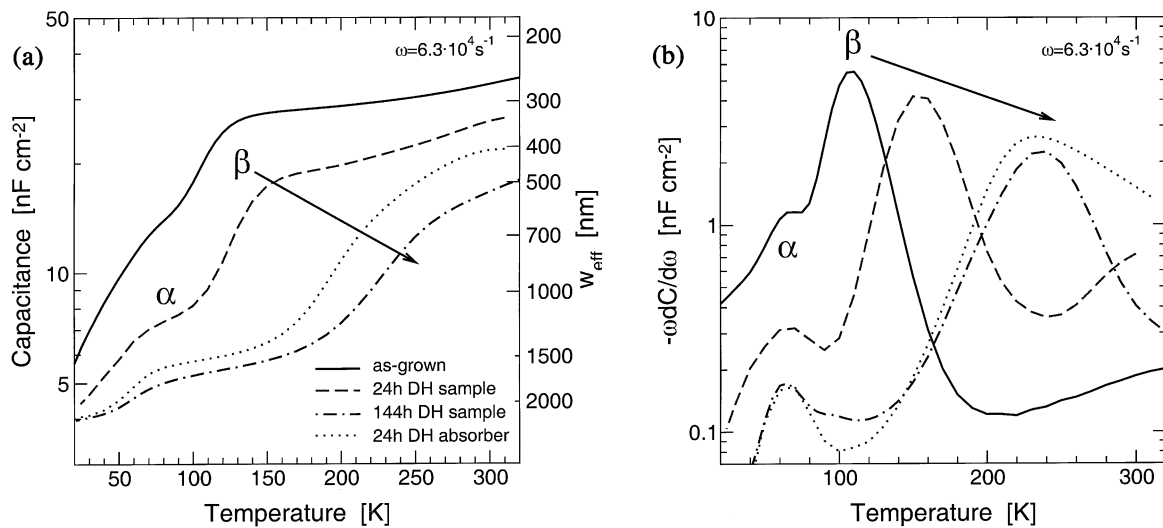


Fig. 2. (a) Capacitance spectrum vs. temperature. Each capacitance step corresponds to a defect state. α is the activation of shallow acceptors, β is the response of states at the window/absorber interface. The interface state, β , shifts to higher temperatures with DH time. The shift of β is also evident for the absorber DH sample. (b) The maximum of each differentiated capacitance spectrum is proportional to the height of the corresponding capacitance step. The latter, in turn, is proportional to the concentration of the states. The concentration of the interface states β is reduced with time elapsed in DH.

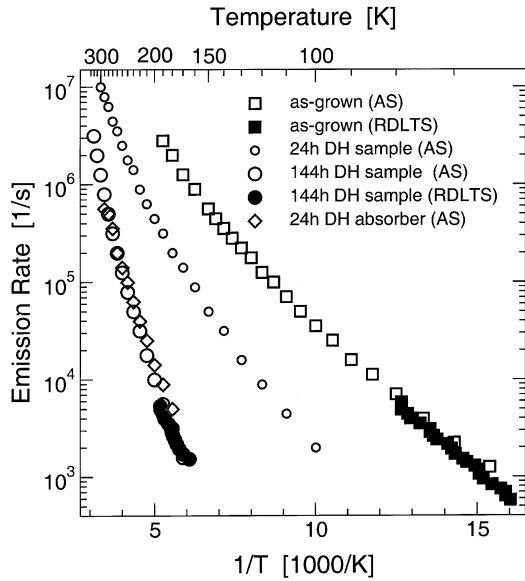


Fig. 3. Arrhenius representation of the admittance data of the interface response, β . The shift shown in Fig. 2 originates from an increase in activation energy (steeper slope), being the difference between the conduction band minimum and the electron Fermi level at the interface, and higher capture cross-section (ordinate intersection) due to DH exposure. Note that the 24-h absorber DH sample and the 144-h DH sample show similar emission rates for β . The slight deviation of the data from straight lines is discussed in the text.

carrier response comes from states at (or close to) the window/absorber interface. For a given excitation frequency, the state β shifts to higher temperatures with DH exposure time. The Arrhenius plot shown in Fig. 3 reveals that both the activation energy, being the difference between the conduction band minimum and the electron Fermi level, and the capture cross-section rise due to DH. A problem arises when determining the activation energy. The data does not follow the straight line in the Arrhenius representation, but deviates systematically. This effect has been previously ascribed to

Table 1
Activation energy ΔE of the interface states

	ΔE [meV]	
	Whole T	High T
as-grown	50	80
2 h DH	85	95
144 h DH	195	315
294 h DH	280	370
438 h DH	315	340
24 h absorber DH	160	180

The columns ‘whole T ’ and ‘high T ’ denote the values of activation energy obtained for the whole temperature range and for the four highest temperatures the states can be seen, respectively. The 24-h DH and the absorber DH sample are of different process runs than the other samples.

the influence of thermally assisted tunneling due to high electric fields at the interface [4]. Tunneling is dominant at low temperatures, only at high temperatures does the emission from trap states become relevant. Accordingly, the activation energies of as-grown and DH samples, fitted in the whole temperature range, yield too low values. In order to minimize this deviation, we use the data in the high-temperature region for the analysis, bearing in mind that these estimates are probably still too low in energy, especially true for emission at low temperatures. A fit of the whole temperature region results in 50 meV activation energy for as-grown samples, whereas the high temperature regime yields 80 meV. For DH samples (144 h), 315 meV activation energy can be read out for high temperatures, instead of 195 meV for the whole range. The values of activation energy for all samples are assembled in Table 1.

The concentration N_{IF} of the interface states, β , (proportional to the capacitance step ΔC [5]) decreases by a factor of two after 144 h of DH. Applying a bias voltage the peak position within the $\omega dC/d\omega$ vs. T spectra remain constant for the as-grown sample indicating a Fermi Level pinning, see Fig. 4. For the DH samples a shift is observed. The decrease of interface density appears to result in an unpinning of the Fermi level. The absorber DH samples show a shift of the activation energy of β with DH time as well. However, in contrast to the DH samples the Fermi level remains pinned.

3. Discussion

We calculated the solar cell output parameters and the band diagram of the ZnO/CdS/Cu(In,Ga)(S,Se)₂ heterostructure using the one-dimensional transport simulation program SCAPS [6]. The parameters used are listed in Table 2 and Table 3, the results are shown in Table 4. The band diagram is shown in Fig. 5. The solid line represents an as-grown cell (parameters corresponding to Table 4, first row), the dashed line corresponds to a DH-treated one (parameters: Table 4, last row). The model takes the following changes due to DH exposure into account: (a) a decrease of conductivity of the window layer, (b) a decrease of the net doping density in the absorber layer, (c) a reduction of the concentration of interface states, and (d) an increase in deep acceptor concentration in the absorber bulk. As the fill factor may be influenced by additional effects like shunts paths or back electrode corrosion which are beyond the scope of this paper we will focus on the increase of activation energy and the decrease of the open circuits voltage.

The increasing resistivity of the ZnO window layer due to DH treatment [1] leads to a raise of the energy difference between conduction band and electron Fermi level, ΔE . However, the corresponding loss in open

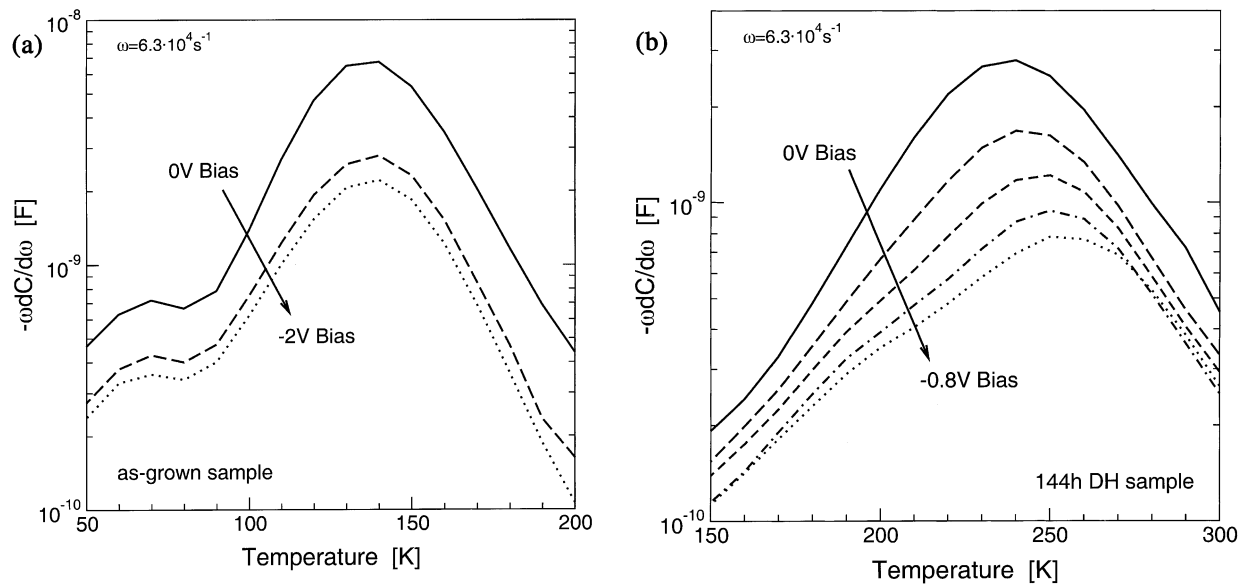


Fig. 4. Differentiated capacitance vs. temperature. The admittance measurements have been performed by applying an external bias. (a) The as-grown samples do not show a shift of the interface response β . This indicates pinning of the Fermi level. (b) For DH samples (here: 144 h) β shows a shift to higher temperatures proportional to the applied reverse bias. The Fermi level pinning is lifted.

Table 2
Parameters of the heterojunction layers used for the SCAPS simulation^a

		p-CIGSSe	n-CdS	n-ZnO
Thickness	[nm]	1000	20	500
Bandgap	[eV]	1.1	2.45	3.4
N_c	[cm ⁻³]	$2 \cdot 10^{18}$	$2 \cdot 10^{18}$	$4 \cdot 10^{18}$
N_v	[cm ⁻³]	$2 \cdot 10^{18}$	$1.5 \cdot 10^{19}$	$9 \cdot 10^{18}$
Mobility μ_n	[cm ² V ⁻¹ s ⁻¹]	50	50	50
Mobility μ_p	[cm ² V ⁻¹ s ⁻¹]	20	20	20
Doping conc.	[cm ⁻³]	$5.5 \cdot 10^{15}$	10^{17}	10^{19}

^a An additional undoped ZnO layer between CdS and n-ZnO has not been taken into account.

circuit voltage is too low to account for the observed DH losses. It has to be mentioned that our results are opposed by Klenk [7], who modeled chalcopyrite solar cells, assuming a recombination velocity of a tenth of the thermal velocity of the charge carriers at the window/absorber interface. A 30% loss of open-circuit voltage is reported when the doping density of the

window layer is reduced to the same value as that of the absorber layer.

The reduced net doping density of the CIGSSe layer alone leads to a decrease of the activation energy ΔE , in contrast to the experiment. In addition to that, the associated loss of cell performance is again much smaller scale than the experimental data.

Changes due to the DH exposure at the interface between absorber and window layer or within the absorber in a surface near region have been reported by different groups: In this paper we have presented the reduction of the concentration of interface states combined with the unpinning of the Fermi level. Using a similar set of samples, Heske et al. [8] observed the forming of S–O bonds at the CIGSSe surface due to DH. Earlier, bonds of oxygen to indium or sodium were reported for CIGSe surfaces exposed to H₂O [9]. Oxygenation of the surface due to In_{Cu}–O bonds was proposed by Cahen and Noufi [10]. However, within the applied SCAPS model the decrease of interface states neither changes the solar cell output parameters

Table 3
Parameters of the defect and interface states used for the SCAPS simulation

Traps in/at	CIGSSe acceptor (N2)	CIGSSe acceptor	CIGSSe/CdS donor
Energy level [meV]	270	550	uniform
Concentration	10^{14} cm ⁻³	10^{15} cm ⁻³	10^{12} cm ⁻² eV ⁻¹
Capture cross-section [cm ²]	$5 \cdot 10^{-14}$	10^{-13}	10^{-15}

Table 4
Results of the SCAPS simulation.

Layer	Parameter changed	V_{oc} [mV]	$\Delta V_{oc}/V_{oc}$	I_{sc} [mA]	η [%]	ΔE [mV]
Reference (as-grown)		562	1	39.2	15.7	97
CIGSSe	doping $2.5 \cdot 10^{15} \text{ cm}^{-3}$	541	0.96	39.6	15.0	85
ZnO	doping 10^{16} cm^{-3}	560	1	39.0	15.4	229
CIGSSe/CdS (IF)	$10^{11} \text{ cm}^{-2} \text{ eV}^{-1}$	562	1	39.2	15.7	97
CIGSSe	acc. $0.55 \text{ eV } 10^{16} \text{ cm}^{-3}$	460	0.82	35.3	10.3	116
CIGSSe	acc. $0.27 \text{ eV } 5 \cdot 10^{15} \text{ cm}^{-3}$	525	0.93	37.8	14.1	114
CIGSSe	both acceptors	460	0.82	34.7	10.2	132
CIGSSe	neutr. $0.55 \text{ eV } 10^{16} \text{ cm}^{-3}$	457	0.81	35.1	10.1	95
CIGSSe	neutral and 0.27 eV acc.	458	0.81	34.8	10.2	112
CIGSSe	don. $0.55 \text{ eV } 10^{16} \text{ cm}^{-3}$	471	0.84	37.2	11.2	87
CIGSSe	donor and 0.27 eV acc.	475	0.85	37.1	11.7	105
CIGSSe doping + IF + both acceptors		448	0.80	34.9	9.8	121
Additionally with ZnO doping		447	0.80	34.3	9.6	314

The output parameters open-circuit voltage V_{oc} , short-circuit current I_{sc} , efficiency η , and activation energy ΔE of β are given to show qualitative trends. The neutral and donor traps in the CIGSSe layer are not additional states, but replacements of the acceptor.

nor the activation energy ΔE that is in contrast to numerical calculation by Rau et al. [11].

As mentioned above, the absorber DH sample shows all the characteristics of DH samples, except for the Fermi level pinning. The CIGSSe bulk therefore is likely to contribute significantly to the impact of DH on the completed device as well. A high concentration of deep acceptors in the absorber bulk can lead to the experimentally found raise of ΔE . One candidate is the acceptor N2 (270 meV), known to increase in density due to DH [2]. In our samples this trap state is not seen

in admittance, only by means of DLTS, which indicates a lower concentration than in cells being processed by co-evaporation [2]. However, in the model, an increase in concentration of these states reduces the SC width, thus enhancing the inversion in contrast to our observations. Thus, N2 alone cannot be responsible for the changes in the CIGSSe bulk, but it might contribute additionally. A midgap acceptor can cause an increase in activation energy of the interface states. The assumed increase in concentration is limited by the onset of significant losses in short-circuit current ($> 10^{16} \text{ cm}^{-3}$)

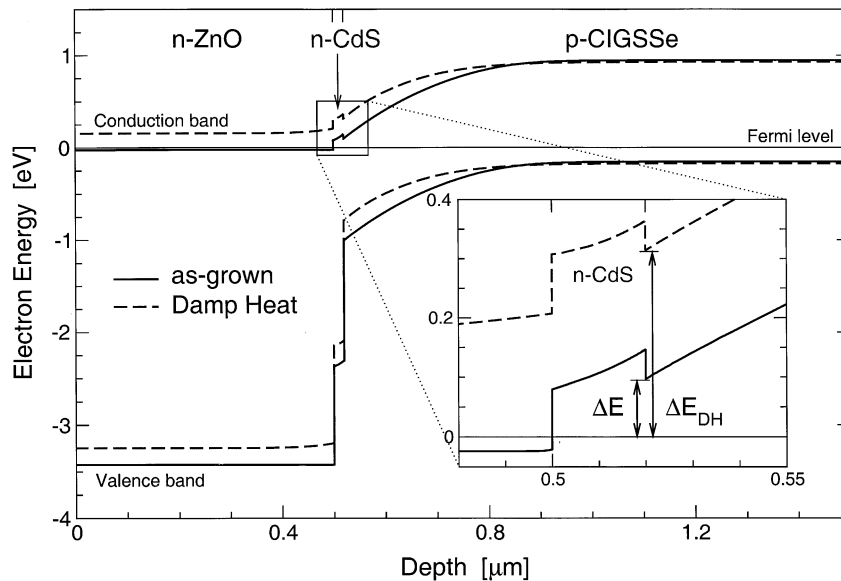


Fig. 5. Band diagram of as-grown (solid line) and DH tested (dashed line) ZnO/CdS/Cu(In,Ga)(S,Se)₂ solar cells calculated using SCAPS. The activation energy ΔE , being the difference between the conduction band minimum and the electron Fermi level at the interface, increases due to DH exposure. The model includes the loss of doping density of absorber and window layer, the reduced concentration of positive charges at the interface, and the influence of a deep acceptor in the absorber bulk.

which were not observed in the experiments. The model calculations show that an increase of the concentration of a deep acceptor to 10^{16} cm^{-3} leads to a decrease of open circuit voltage even larger than observed. The increase of activation energy ΔE lies within the range observed for the absorber DH sample. Modeling the shift of ΔE beyond 300 meV measured after the DH treatment of completed cells with CdS and ZnO, however, requires the additional effect of the increase of ZnO resistivity.

4. Conclusions

Applying admittance spectroscopy and DLTS we observe the consequences of damp heat exposure of solar cells based on Cu(In,Ga)(S,Se)_2 . Changes of the electrical characteristics occurring, only for unencapsulated cells — in particular a decrease of the open circuit voltage — originate from a combination of different effects. The experiments show a reduction of doping density of the absorber layer, an increase of the energetic difference ΔE between conduction band and electron Fermi level and a decrease of interface states. The increase of ΔE and the decrease of open circuit voltage can be modeled by the introduction of deep acceptor states alone in the case of the absorber DH sample and

with an additional increase of ZnO resistivity for DH treated devices. The cases studies reported here with SCAPS have to be extended to include interactions between ZnO resistivity, interface density and bulk properties. The impact of defect states in the CdS layer should be investigated, too.

References

- [1] J. Wennerberg, J. Kessler, M. Bodegård, L. Stolt, Proceedings of the second World Conference on Photovolt. Energy Conv., 1998, p. 116.
- [2] M. Schmidt, D. Braunger, R. Schäffler, H.W. Schock, U. Rau, Thin Solid Films 361–362 (2000) 283.
- [3] V. Probst, W. Stetter, W. Riedl, H. Vogt, M. Wendl, H. Calwer, S. Zweigart, K.D. Ufert, B. Freienstein, H. Cerva, F. Karg, Thin Solid Films 387 (2001) 262.
- [4] P. Zabierowski, M. Igalson, Thin Solid Films 361–362 (2000) 268.
- [5] E.H. Nicollian, A. Goetzberger, Appl. Phys. Lett. 7 (1965) 216.
- [6] A. Niemegeers, M. Burgelman, Proceedings of the twenty-fifth IEEE Photovolt. Spec. Conference, 1998, p. 901.
- [7] R. Klenk, Thin Solid Films 387 (2001) 135.
- [8] C. Heske, U. Groh, E. Umbach, S. Zweigart, F. Karg, (unpublished).
- [9] C. Heske, G. Richter, Z. Chen, R. Fink, E. Umbach, W. Riedl, F. Karg, J. Appl. Phys. 82 (1997) 2411.
- [10] D. Cahen, R. Noufi, Solar Cells 30 (1991) 53.
- [11] U. Rau, D. Braunger, R. Herberholz, H.W. Schock, J.F. Guillemoles, L. Kronik, D. Cahen, J. Appl. Phys. 86 (1999) 497.